ACS Chemical Neuroscience

Research Article

pubs.acs.org/chemneuro

Direct High Affinity Interaction between Aβ42 and GSK3α Stimulates Hyperphosphorylation of Tau. A New Molecular Link in Alzheimer's Disease?

Christopher J. Dunning,[†,‡,∥] Gavin McGauran,[§,∥] Katarina Willén,[‡] Gunnar K. Gouras,[‡] David J. O'Connell,[*,§] and Sara Linse[*,†]

[†]Department of Biochemistry and Structural Biology, Chemical Centre, Lund University, P O Box 124, SE22100 Lund, Sweden

[‡]Department of Experimental Medical Science, Lund University, SE22100 Lund, Sweden

[§]School of Biomolecular & Biomedical Science, Conway Institute, University College Dublin, Belfield, Dublin 4, Ireland

Supporting Information

ABSTRACT: Amyloid β peptide (Aβ42) assemblies are considered central to the development of Alzheimer's disease, but the mechanism of this toxicity remains unresolved. We screened protein microarrays with on-pathway oligomeric Aβ42 to identify candidate proteins interacting with toxic Aβ42 species. Samples prepared from Alexa546-Aβ42 and Aβ42 monomers at 1:5 molar ratio were incubated with the array during a time window of the amyloid fibril formation reaction during which the maximum number of transient oligomers exist in the reaction flux. A specific interaction was detected between Aβ42 and glycogen synthase kinase 3α (GSK3α), a kinase previously implicated in the disease pathology. This interaction was validated with anti-GSK3α immunoprecipitation assays in neuronal cell lysates. Confocal microscopy studies further identified colocalization of Aβ42 and GSK3α in neurites of mature primary mouse neurons. A high binding affinity (K_D = 1 nM) was measured between Alexa488-Aβ42 and GSK3α in solution using thermophoresis. An even lower apparent K_D was estimated between GSK3α and dextran-immobilized Aβ42 in surface plasmon resonance experiments. Parallel experiments with GSK3β also identified colocalization and high affinity binding to this isoform. GSK3α-mediated hyperphosphorylation of the protein tau was found to be stimulated by Aβ42 in *in vitro* phosphorylation assays and identified a functional relationship between the proteins. We uncover a direct and functional molecular link between Aβ42 and GSK3α, which opens an important avenue toward understanding the mechanism of Aβ42-mediated neuronal toxicity in Alzheimer's disease.

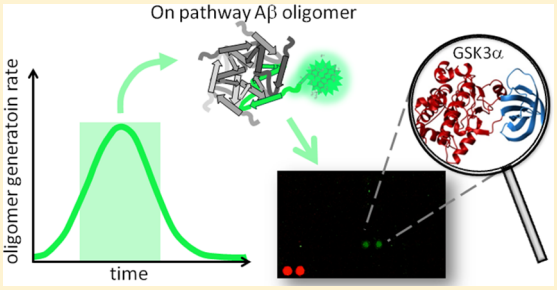

KEYWORDS: *Interactome, signaling, target protein, amyloid beta, microarray screen*

Alzheimer's disease (AD) is the major neurodegenerative disease leading to dementia. Next to the suffering of those afflicted by the disease, the costs for society are escalating as the number of affected individuals is increasing.[1] There is a pressing need to determine the underlying molecular processes of the disease to make it possible to design early diagnostics and future therapy.[2] Brain function is severely perturbed in AD patients due to dysfunction and loss of neurons, but the molecular mechanisms leading to these changes are poorly understood. Pathological hallmarks of AD include neurofibrillar tangles of protein tau and extracellular plaques containing fibrils of amyloid β peptide (Aβ). Among the suspect molecular processes leading to AD are hyperphosphorylation of the protein tau and self-assembly of Aβ into fibrillar and oligomeric aggregates.[3,4]

In vivo, proteolysis of the amyloid precursor protein (APP) leads to several Aβ length variants, including the disease-linked Aβ42 (Figure 1A). Mutations in APP that affect Aβ42 production rate or aggregation process cause familial forms of early onset AD,[5−7] and a genetic correlation between AD and the apoε4 allele for apolipoprotein E has been found.[8] Still the majority of AD cases are sporadic.

In vitro mechanistic studies have found that the aggregation of Aβ42 peptide into oligomeric and fibrillar assemblies is governed by an autocatalytic reaction, in which the dominant route to oligomer formation relies on nucleation of monomers on fibril surfaces.[9,10] At all time points, the reaction is dominated by monomeric or fibrillar species, while oligomeric species are transient in nature and represent a minor fraction[9−11] of the total peptide concentration. On a macroscopic level, the fibril concentration as a function of time displays a sigmoidal curve with a lag phase, a growth phase and a final plateau (Figure 1B). The monomer concentration follows an inverse sigmoidal curve (Figure 1B). The oligomer concentration is highest at the end of the lag phase and toward

Received: October 5, 2015
Accepted: November 30, 2015
Published: November 30, 2015

DOI: 10.1021/acschemneuro.5b00262
ACS Chem. Neurosci. 2016, 7, 161−170

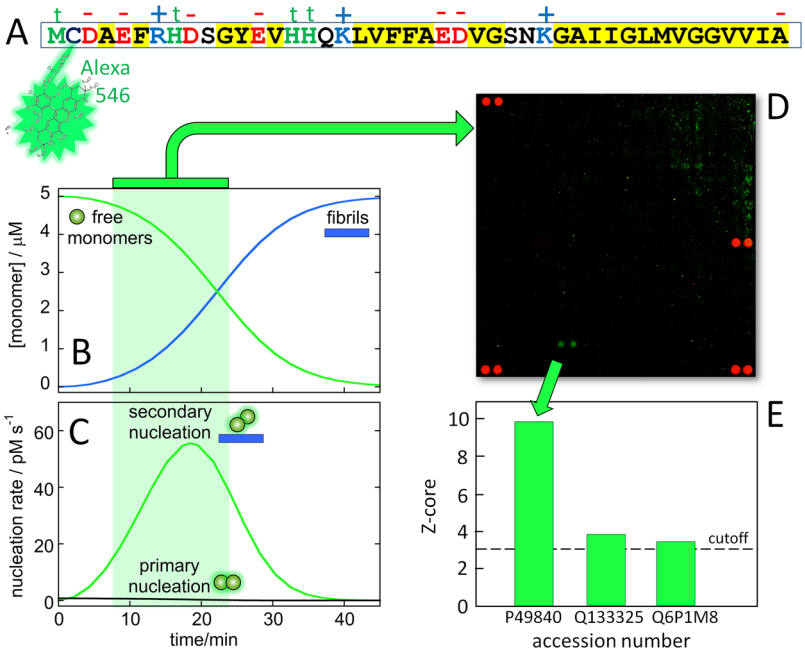

Figure 1. Principles of protein array screening to find interaction partners of on-pathway Aβ42 oligomers. (A) Amino acid sequence of Aβ(MC1−42) with the Alexa546 chromophore attached to the cysteine residue added at the N-terminus. Hydrophobic residues are on yellow background, while t, + , and − indicate residues that are titrating (t) and positively (+) and negatively (−) charged around neutral pH. (B) Fibril formation as a function of time starting from 5 μM monomeric Aβ42 in physiological salt buffer at pH 8.0. The fibril concentration is shown in blue and monomer concentration in green. (C) Nucleation rates during the same aggregation reaction, calculated from concentrations and rate constants determined in physiological salt (unpublished experiment). The rate of primary nucleation is shown in black, and the rate of secondary nucleation in green. The time window during which the solution was incubated with the protein array is shown as a shaded green area in panels (B) and (C). (D) Example of a subarray with guiding spots in red, and the spots of a putative interaction in green. (E) *Z*-scores of three duplicate spots that were found above the cutoff when the array was probed with on-pathway Aβ42 assemblies.

the midpoint of the growth phase. The vast majority of these oligomers originate from secondary nucleation of monomers on fibril surfaces. Primary nucleation dominates at the very earliest stage of a reaction starting from pure monomer (black line close to baseline in Figure 1C). Because of rapid elongation, the fibril concentration is already after a few minutes of the reaction high enough for secondary nucleation to take over as the dominant nucleation process (Figure 1C, ref 12). Because the rates of secondary nucleation as well as elongation are dependent on concentrations of both fibril and monomer, the rates of nucleation as well as fibril multiplication is highest during the growth phase, where both species are present at significant concentrations.

With an aim to discern cellular pathways responsible for Aβ42 oligomer toxicity, we here use high-content protein microarrays in an unbiased search for interaction partners of Aβ42 oligomers that form during an ongoing aggregation reaction. Searches for molecular interaction partners of toxic Aβ42 species by affinity chromatography, yeast-2-hydrid approaches, pull-down assays and protein array screening are challenged by the high surface activity of Aβ42 and the transient nature of the toxic species. The surface activity of Aβ42 arises from its amphiphatic amino acid sequence (Figure 1A), and the peptide has a strong tendency to adsorb to many kinds of surfaces.[13] This may lead to strong background signal or false positives, but can be addressed by careful choices of surface blockers or negative controls. Another challenge comes from recent insights that the toxicity is mediated by transient oligomeric species formed during the aggregation reaction, most prominently in a reaction involving both monomeric and fibrillar species.[9,14] This challenge has been addressed using trapped oligomers, for example, using a disulfide-linked Aβ42 variant that forms relatively large oligomers (protofibrils) that do not convert to fibrils.[15,16]

As an alternative strategy, we here use on-pathway samples and incubate protein arrays with these samples during a time-window of the reaction during which a finite fraction of transient oligomeric species are formed and coexist with mainly monomers and fibrils in the reaction flux (Figure 1B,C; refs 9−12). A third challenge arises from the tendency of large aggregates to sediment, which might lead to false positives in array screening. We overcome this obstacle by placing the array on top of the liquid so that only diffusible assemblies may reach its surface. While previous searches for Aβ target proteins in human plasma, cerebrospinal fluid, and soluble brain extracts have reported mainly extracellular proteins,[8,15−18] and cell surface receptors,[19−21] we identify here an intracellular target of oligomeric Aβ42: glycogen synthase 3α. A high affinity interaction is validated by thermophoresis, surface plasmon resonance, and immunoprecipitation. Colocalization in mature mouse primary neurons is studied by confocal microscopy, and *in vitro* kinase assays are used to study a potential functional consequence of the interaction.

RESULTS AND DISCUSSION

Array Screening with On-Pathway Aβ42. We used on-pathway Aβ42 samples to probe protein arrays with >9000 human proteins (Figure 1D) in an unbiased search for protein interaction partners of transient Aβ42 oligomers, which may provide new keys toward the molecular origin of Aβ42 oligomer toxicity. The design of the study relies on detailed knowledge of the reaction mechanism (refs 9−12; Figure

DOI: 10.1021/acschemneuro.5b00262
ACS Chem. Neurosci. 2016, 7, 161−170

1B,C), the high affinity of Aβ42 for many surfaces[13] requiring stringent surface blocking, and the recent finding of unperturbed reaction kinetics when samples are doped with a minor fraction of Aβ42 with N-terminally incorporated fluorophore.[22]

To enable fluorescence detection, we used the Aβ(MC1−42) variant with a cysteine residue incorporated just prior to Asp1 to allow for site-specific labeling with Alexa546 at the N-terminus. We chose to label the N-terminus because it is flexible not only in Aβ42 monomers, but also in Aβ42 oligomers and fibrils.[23,24] We used a 1:5 mixture of Alexa546-Aβ(MC1−42) and Aβ(M1−42) monomers separately isolated by gel filtration just prior to the array experiment. The monomer mixture was preincubated for 8 min at 37 °C to initiate the aggregation reaction, which was continued for another 15 min in contact with a protein array (Figure 1). The array experiment was thus designed to sample the end of the lag phase and start of the growth phase, during which periods a very large number of nucleation and oligomer formation events occur.[11] During this time window, secondary nucleation totally dominates oligomer generation (Figure 1C). The microscope slide with the array was placed face-down on top of the solution to avoid false positives due to sedimenting fibrils.

We identify one positive interaction with glycogen synthase kinase 3 alpha (GSK3α) (Figure 1E). Two other proteins were found very close to this statistical cutoff (Figure 1E, Table 1).

Table 1. Putative Aβ42 Targets Observed above the Intensity Threshold of 3.0 after Incubation during the Time Window Shown in Figure 1 of the Main Text

UniProt	gene	protein	intensity	no. of residues
P49840	GSK3A	glykogen synthase kinase 3α	9.86	483
Q13325	IFIT5	interferon-induced protein with tetratricopeptide repeats 5	3.89	482
Q6P1M8	ASXL1	ASXL1 protein	3.43	84

The significant signal for GSK3α combined with lack of signal for the vast majority of the array spots is a remarkable finding. It suggests that transient Aβ42 oligomers have relatively few high-affinity targets with slow enough dissociation to sustain the washing period of 10 min before imaging. Moreover, it shows that the blocking solution used (5% milk) is sufficient to prevent unspecific adsorption of Aβ42 monomers, oligomers, or fibrils. The signal obtained for Aβ42 bound to GSK3α is relatively weak. However, this is in line with the low concentration of transient oligomers during the reaction (refs 9,10; Figure 1B). The array experiment was repeated during a later stage of the reaction, when the sample was dominated by fibrils, in which case only two other weak signals close to cutoff were detected (Table 2).

Validation. The array study provides a first clue to a direct high affinity interaction between Aβ42 and GSK3α. We used four independent methods to validate this interaction with purified proteins, cell lysates or in neurons: (1) surface plasmon resonance (SPR) analysis with purified proteins (Figure 2), (2) thermophoresis with purified proteins (Figure 3), (3) pull-down assays with cell lysates, monoclonal antibodies, and IR800-Aβ42 (Figure 4), and (4) confocal fluorescence microscopy with fluorescently labeled monoclonal antibodies (Figure 5).

Table 2. Putative Aβ42 Targets Observed above the Intensity Threshold of 3.0 after Incubation of an Array with a Fibrillar Sample

UniProt	gene	protein	intensity	no. of residues
Q8IUC8	GALNT13	polypeptide *N*-acetylgalactosaminyl-transferase 13	3.40	556
A6ZKI3	FAM127A	protein FAM127A	3.09	113
or		or		or
O15255		CAAX box protein 1		209

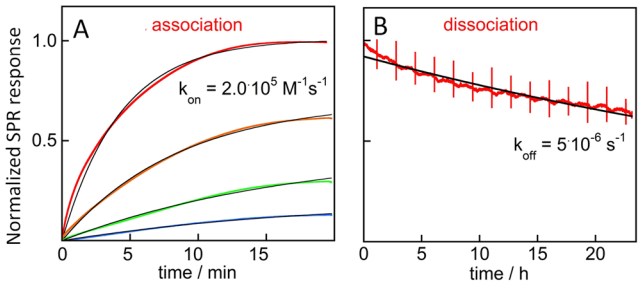

Figure 2. SPR analysis of the interaction between Aβ42 and GSK3α. (A,B) SPR data at 25 °C. GSK3α was injected at 20 nM (red), 10 nM (orange), 5 nM (green), and 2.5 nM (blue) for 20 min over a dextran-coated CM5 sensor chip with immobilized Aβ42 (A) followed by buffer flow for 24 h (B). The association phase data are baseline subtracted and normalized relative to curve for the highest concentration, and each curve shown is the average over three repeats. The dissociation phase data is the average over three repeats, baseline subtracted and normalized to start at 1.0. The vertical lines at regular intervals are pump changes. The fitted curves for a 1:1 binding reaction are shown in black.

Surface Plasmon Resonance. The SPR analysis (Figure 2A,B) indicates a high affinity interaction between purified GSK3α and Aβ42 immobilized in a dextran matrix of a sensor chip surface. The dissociation is too slow for its rate constant to be accurately determined. Although the average data over three repeats (Figure 2B) can be fitted using $k_{off} = 5 \times 10^{-6}$ s^{-1}, the baseline is not reached during the 24 h time frame of the experiment, and there are problems with instrument drift and reproducibility over such long periods, it is more safe to estimate a limiting value for k_{off} ($k_{off} \leq 2 \times 10^{-5}$ s^{-1}). Together with the fitted association rate constant ($k_{on} = 2 \times 10^5$ M^{-1} s^{-1}), we estimate a limit for an apparent equilibrium dissociation constant ($K_D \leq 100$ pM). During immobilization Aβ42 was applied as a monomer; however, after coupling to the dextran matrix, Aβ42 most likely exists as a mixture of oligomeric and monomeric species. It is also possible that immobilized peptides exchange between these states. The measured binding parameters may thus represent binding to Aβ42 monomer or oligomer or a weighted average over several species in a dextran matrix. Control experiments were performed with EF-hand 1 from calbindin D_{9k} coupled to the sensor chip. This peptide has similar size as Aβ42 and similar net charge, but no binding was observed during the injection of 20 nM GSK3α (Figure S1A).

Thermophoresis. The thermophoresis data (Figure 3) indicate that a relatively high affinity interaction (K_D = 1 nM) develops over time between GSK3α and Aβ42 in solution. This suggests that the observed interaction is with an aggregated form of Aβ42 (oligomer or fibril). The time frame of oligomer formation is much longer in the thermophoresis experiment

DOI: 10.1021/acschemneuro.5b00262
ACS Chem. Neurosci. 2016, 7, 161−170

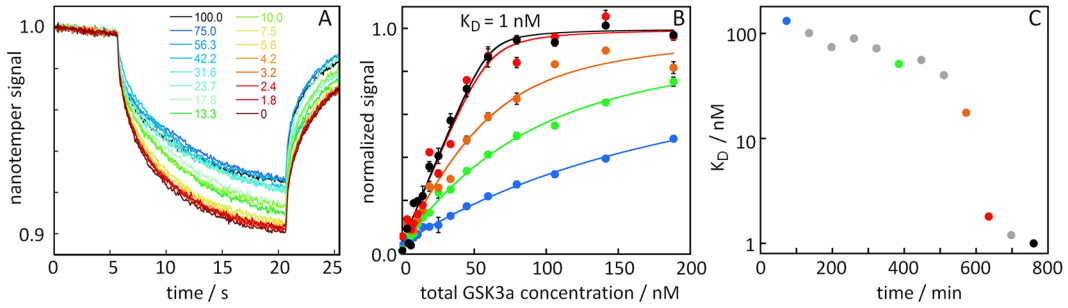

Figure 3. Thermophoresis analysis of the interaction between Aβ42 and GSK3α. (A) Thermophoresis time traces at 37 °C for the 16 capillaries containing solutions with 60 nM Aβ42 alone and varying GSK3α concentrations. The example shown is recorded after 635 min, and the GSK3α concentrations are listed in % of the highest (188 nM GSK3α). (B) Normalized thermophoresis signal (averages and standard deviations over 5 repeats) is shown for a selected set of incubation times: 30 min (blue), 385 min (green), 572 min (orange), 635 min (red), and 800 min (black). The fitted curves for a 1:1 binding reaction are shown as solid lines for K_D = 1.0 nM (black), 1.8 nM (red), 18 nM (orange), 51 nM (green), and 132 nM (blue). (C) The fitted K_D values as a function of incubation time. The time points shown in blue, green, orange, red, and black use the same color codes as in panel (B).

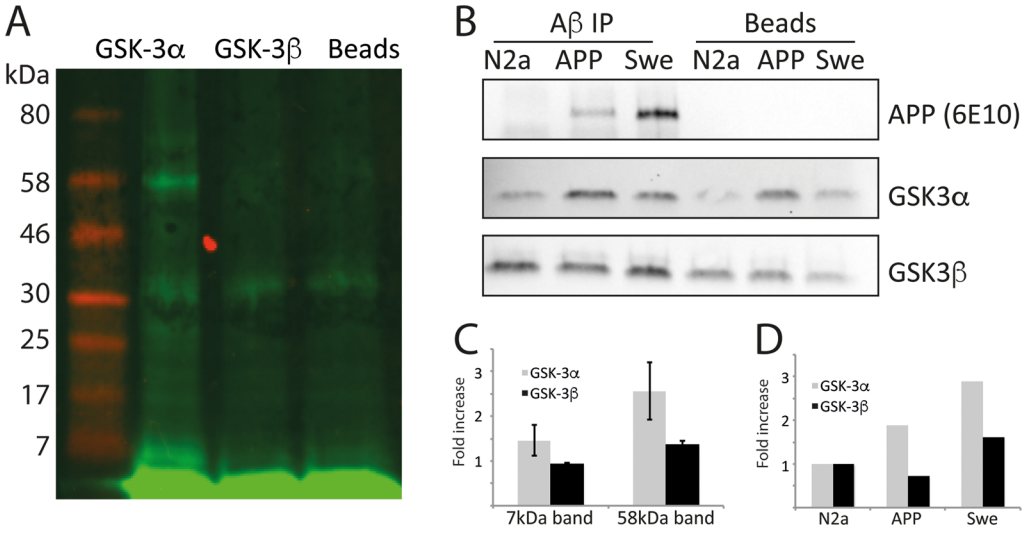

Figure 4. Immunoprecipitation study of the interaction between Aβ42 and GSK3α. (A,B) Immunoprecipitation assay in neuronal cell lysates with IR800-labeled Aβ(MC1−42) and bead-conjugated monoclonal antibodies against GSK3α. (A) Immunoblot scan from experiments with bead-conjugated monoclonal antibodies against GSK3α, GSK3β, or beads alone. IR800-labeled Aβ(MC1−42) is seen in green and the M_w standards in red. (B) Immunoprecipitation assay in neuronal cell lysates with bead-conjugated monoclonal antibodies against Aβ (4G8), and Western blot using monoclonal antibodies against GSK3α or APP. The cell lines were naïve N2A cells, or cells overexpressing human APP or human APP with the so-called Swedish mutation (Swe) leading to 10-fold enhanced production of Aβ42. Probing with 6E10 revealed the presence of full length APP only. (C) Quantification of IR-800 signal for the 7 and 58 kDa bands relative to intensity obtained with naked beads (n = 3). Error bars show SEM. (D) Quantification of GSK3 immunoprecipitation from APP neuroblastoma cell lines. Background from beads only was subtracted from the IP signal and fold increase plotted relative to signal in the N2a control line.

(Figure 3) compared to the array study (Figure 1), due to the difference in total peptide concentration (60 nM versus 5 μM). Both thermophoresis in solution and SPR at a surface detect a high affinity interaction between GSK3α and Aβ42. The lower K_D value as estimated by SPR may be due to surface effects in the SPR measurement, which typically overestimates binding affinities in comparison with in-solution assays. Control thermophoresis experiments reveal no high affinity interaction between calbindin D9k and Aβ42, showing that the observed changes in thermophoretic properties of Aβ42 are not merely due to the presence of another protein (Figure S1B).

Immunoprecipitation. The pulldown assays utilized a monoclonal antibody against GSK3α and IR800-labeled Aβ42 to study the interaction in a complex fluid representing an in-cell environment. After isolating GSK3α from SH-SY5Y cell lysates using bead-coupled anti-GSK3α antibody, IR800-labeled Aβ42 was added and a GSK3α -Aβ42 interaction confirmed using IR fluorescence imaging (Figure 4A). The interaction between Aβ42 and GSK3α sustains multiple washing steps over a period of ca. 30 min, which means that the interaction is of relatively high affinity and has a low off-rate. The assay is complicated by the high surface affinity of Aβ42. The beads were therefore blocked with 5% milk and control experiments were performed with beads alone and beads coupled to anti-GSK3β antibody. For GSK3α, two gel bands of apparent M_w of ca. 7 and ca. 58 kDa are significantly stronger than other bands, and when the intensity of the beads alone is subtracted, reveals an increase in IR800 intensity of 1.4 ± 0.34 for the 7 kDa band and 2.56 ± 0.63 for the 58 kDa band. In contrast, the corresponding band in the GSK3β lane reveals little to no increased binding of IR800-labeled Aβ42 (7 kDa: 0.93 ± 0.03, 58 kDa: 1.36 ± 0.09) (Figure 4C). The M_w of IR800-labeled Aβ42 is ca. 5.6 kDa and GSK3α ca. 51 kDa. The higher band is intriguingly sharp and corresponds to ca. 10 IR800-labeled

DOI: 10.1021/acschemneuro.5b00262
ACS Chem. Neurosci. 2016, 7, 161−170

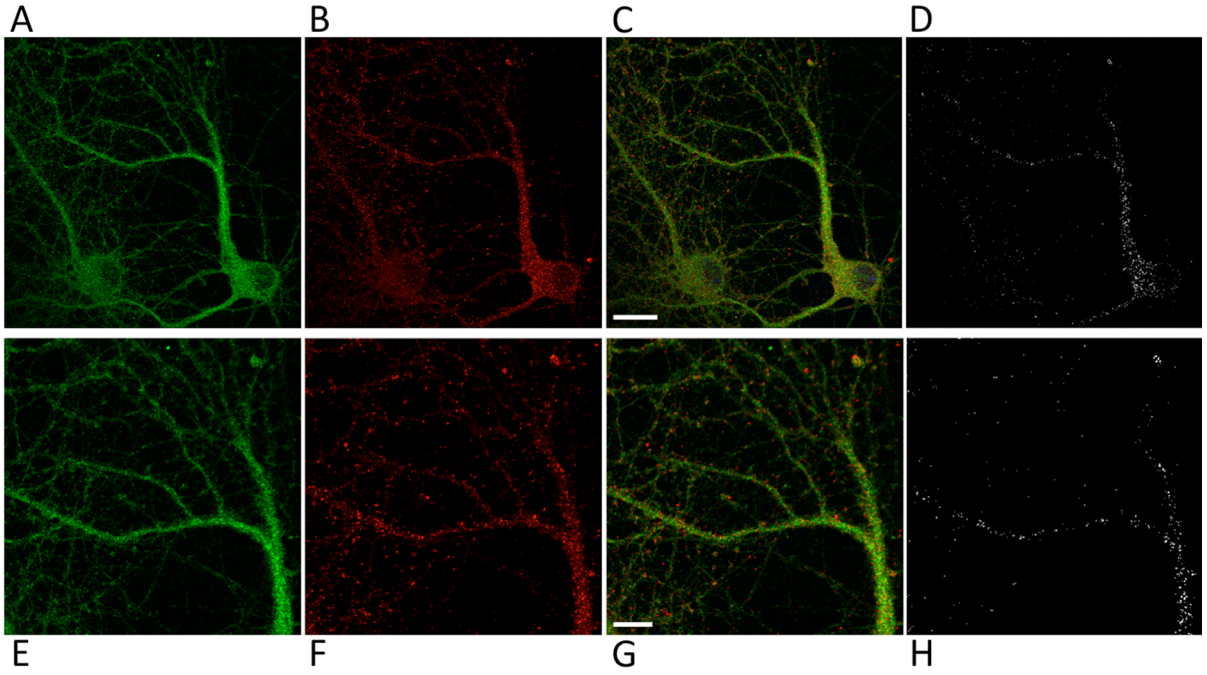

Figure 5. Confocal fluorescence microscopy shows colocalization of GSK3α and Aβ42 in primary mouse neurons. Images from a single z-plane of primary mouse neurons at 19 DIV using monoclonal antibodies against GSK3α (green, panels A,C,E,G) and Aβ42 (red, panels B,C,F,G) and nucleus (blue DAPI stain, panel C). In panels (C) and (G), colocalization of GSK3α and Aβ42 is observed as yellow areas. Panels (D) and (H) show colocalization (white) of GSK3α and Aβ42 and was determined by using ImarisColoc, which shows only pixels with relative colocalization. (A–D) Overview image of one typical neuron. Scale bar = 20 μm. (E–H) Zoom in images of the neurites. Scale bar = 10 μm.

Aβ42 or one IR800 labeled Aβ42 plus one GSK3α, or may represent some SDS induced oligomer of a lower M_w state.[25]

In a second set of experiments, beads with a monoclonal antibody against Aβ (4G8) were used in a coimmunoprecipitation experiment, where Aβ42 was immunoprecipitated from either control N2a cells or N2a cells overexpressing amyloid precursor protein wildtype or with Swedish mutation[26] before detecting GSK3α and GSK3β via Western blot (Figure 4B). Again, higher intensities were found with GSK3α when compared to either GSK3β or beads alone (Figure 4D). It is also apparent that with more amyloid beta production due to the Swedish mutation, we see increased levels of GSK3α coprecipitating.

Confocal Microscopy. Confocal microscopy was used to study the distribution of Aβ42 and GSK3α in mature primary mouse neurons (Figure 5), and we detect both Aβ42 and GSK3α in a punctate pattern along the neurites. Still, in most parts of the neurons the two proteins do not coexist, in line with the relatively weak specific signal observed in the IP experiments. Because of its resolution limit, the confocal microscopy data does not tell whether there is any direct contact or high affinity binding between the two proteins, but does provide evidence of colocalization of Aβ42 and GSK3α.

Tau Phosphorylation. We next asked whether Aβ42 directly stimulates GSK3α. We used an *in vitro* kinase assay with purified GSK3α and tau in a buffer system with ATP. The assay was performed in the absence and presence of 5–500 nM Aβ42, which had been preincubated at 5 μM for a short time to initiate the formation of transient oligomers before dilution into the reactions. Tau phosphorylation by GSK3α was detected by Western blot using a phospho-tau specific antibody recognizing phosphorylation of Ser396 (Figure 6). In the presence of Aβ42, we find a factor of 6.3($\pm$2.4) stronger signal with GSK3α compared to no enzyme, with no variation over the Aβ42

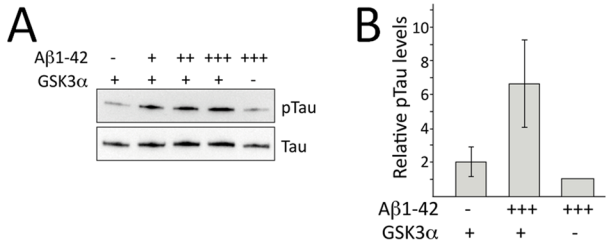

Figure 6. Tau phosphorylation assay. (A) Examples of tau gel bands from Western blot imaging after kinase assay reaction in the absence (−) and presence of Aβ42 at 5 nM (+), 50 nM (++), and 500 nM (+++), and absence (−) or presence of GSK3α (+). (B) Quantification of tau phosphorylation in the presence (+++) or absence (−) of 500 nM Aβ42, and absence (−) or presence of GSK3α (+). Levels of pTau were compared to reactions performed in the absence of GSK3α. Data shown are Mean $\pm$ SEM (n = 3).

concentration range studied in line with the high affinity of the interaction. In the absence of Aβ42 we find a factor of 1.9($\pm$0.8) stronger signal with GSK3α compared to no enzyme. Thus, Aβ42 was found to increase GSK3α activity in terms of tau phosphorylation by a factor of 3 under the conditions of the assay.

A New Molecular Link in Alzheimer's Disease? The finding of GSK3α as the top candidate in an unbiased search for putative interaction partners of transient Aβ42 oligomers, its validation as a high affinity interaction, and the observed stimulation of tau hyperphosphorylation by GSK3α in the presence of Aβ42 are striking results given the strong connection found previously between GSK3 and Alzheimer's disease; as recently reviewed.[27−30] GSK3 has been investigated by others as a critical molecular link between the two histopathological hallmarks of the disease: Aβ plaques and neurofibrillary tau tangles. Hyperactivated GSK3 has been

DOI: 10.1021/acschemneuro.5b00262
ACS Chem. Neurosci. 2016, 7, 161−170

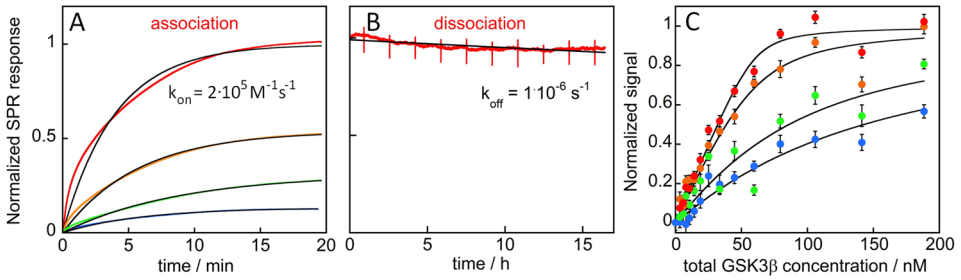

Figure 7. SPR and thermophoresis analysis of the interaction between Aβ42 and GSK3β. (A,B) SPR data at 25 °C. GSK3β was injected at 20 nM (red), 10 nM (orange), 5 nM (green), and 2.5 nM (blue) for 20 min over a dextran-coated CM5 sensor chip with immobilized Aβ42 (A) followed by buffer flow for 24 h. (B) Fitted curves for a 1:1 binding reaction are shown in black. (C) Normalized thermophoresis signal for 16 capillaries containing solutions with 60 nM Aβ42 alone and varying GSK3α concentrations (averages and standard deviations over 5 repeats) is shown for a selected set of incubation times: 30 min (blue), 385 min (green), 572 min (orange), and 635 min (red). The fitted curves for a 1:1 binding reaction are shown as solid black lines for K_D = 2.3, 16, 65, and 110 nM.

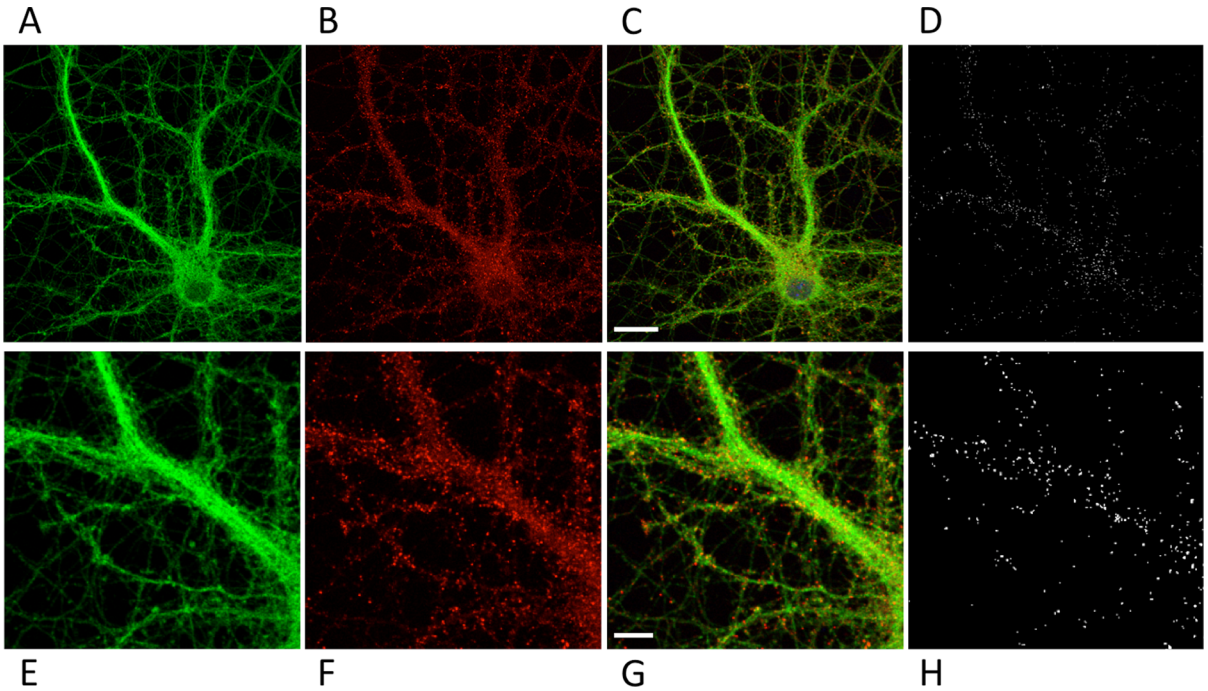

Figure 8. Confocal fluorescence microscopy shows colocalization of GSK3β and Aβ42 in primary mouse neurons. Images from a single z-plane of primary mouse neurons at 19 DIV using monoclonal antibodies against GSK3β (green, panels A,C,E,G) and Aβ42 (red, panels B,C,F,G) and nucleus (blue DAPI stain, panel C). In panels (C) and (G), colocalization of GSK3α and Aβ42 is observed as yellow areas. Panels (D) and (H) show colocalization (white) of GSK3α and Aβ42 and was determined by using ImarisColoc, which shows only pixels with relative colocalization. (A–D) Overview image of one typical neuron. Scale bar = 20 μm. (E–H) Zoom in images of the neuronal structures. Scale bar = 10 μm.

linked to sporadic as well as familial AD, suggesting a crucial role of this enzyme in AD pathogenesis. The discovery presented here of a direct interaction of Aβ42 with GSK3α, leading to stimulation of kinase activity, provides a new route toward resolving how this molecular link affects the etiology of the disease.

Glycogen Synthase Kinase 3. GSK3 is a central and multifunctional kinase with important roles in synaptic plasticity, memory, and learning.[31,32] Its two isoforms (or rather paralogues[27]), GSK3α and GSK3β, can phosphorylate over 100 known substrates in addition to glycogen synthase. One important substrate is the protein tau, the phosphorylation of which is thought to be a critical step in AD pathogenesis.[3] Indeed, GSK3β was called tau protein kinase 1 (TPK1) before gene cloning and sequencing revealed that the two proteins are the same.[33] The involvement in AD has been studied most extensively for GSK3β, but specific contributions of GSK3α and GSK3β have been inferred from siRNA and knockdown studies.[27,29,34,35] GSK3α seems to enhance Aβ production through γ-secretase stimulation,[34,35] which has been proposed to be due to "interaction with an unidentified protein".[35] Aβ42 uptake and accumulation in neurons, has been observed to lead to GSK3 activation.[36−38] Studies in primary hippocampal neurons suggest that Aβ42 accumulations invoke an intracellular cascade that culminates in caspase and GSK3 activation; however, the molecular mechanisms that link toxicity of Aβ42 oligomers to GSK3 activation remain unknown.[38]

Glycogen Synthase Kinase 3β. GSK3α and GSK3β share 83% sequence identity in the 370-residue kinase domain (Figure S2). In addition to the kinase domain, GSK3α has a 90 residue N-terminal extension, in which residues 15−25 of GSK3α are 82% identical to residues 2−13 of the 27 residue N-terminal extension of GSK3β. Although GSK3β is present on the protein array, there can be many reasons for a protein not

DOI: 10.1021/acschemneuro.5b00262
ACS Chem. Neurosci. 2016, 7, 161−170

emerging as a putative hit including lower amount spotted, lower level of correctly folded protein in the spot, and so forth. A few control experiments were therefore performed using SPR (Figure 7A,B), thermophoresis (Figure 7C) and confocal fluorescence microscopy (Figure 8), indicating that oligomeric Aβ42 interacts and co-localizes also with GSK3β.

CONCLUDING REMARKS

The direct interaction discovered between oligomeric Aβ42 and GSK3α, a kinase at the cross-roads of many intracellular signaling pathways, provides a new molecular link that may have implications for toxicity in Alzheimer's disease. It is an intriguing finding in light of the reported correlations between Aβ42 uptake or production and GSK3α activity in neurons.[34−38]

Our findings of a direct molecular link between Aβ42 and GSK3α may open up new directions for studies of early molecular events in the disease. Future studies of the interaction between Aβ42 and GSK3α may aim to identify the binding site, to find factors that modulate the affinity, and to provide a deeper understanding of kinase activation and its consequences; the results may further our understanding of Alzheimer's disease and provide a fundament for development of future therapeutic intervention or diagnosis.

METHODS

Chemicals. All chemicals were of the highest purity available. Alexa Fluor 488 maleimide and Alexa Fluor 546 maleimide were purchased from Life Technologies. IRDye 800RD Infrared Dye maleimide was purchased from LI-COR, and ATP from Sigma-Adrich.

Expression and Purification of Aβ Peptides. Aβ(M1−42) and Aβ(MC1−42) were expressed in *Escherichia coli* from synthetic genes with *E. coli* optimized codons. The gene for Aβ(MC1−42) was produced by PCR using as a template the PetSac vector with Aβ(M1−42) gene,[39] the start primer GCGTAGGGTCGACATATG**TGC**GACGCTGAATTCCGTCACG with an introduced Cys codon (**TGC**) and the Aβ42stop primer.[39] The gene was cut with NdeI and SacI and cloned into PetSac vector, a derivative of Pet3a. Aβ(M1−42) was purified as described.[39] Briefly, *E. coli* cells were sonicated three times in 10 mM Tris/HCl, 1 mM EDTA, pH 7.5 using centrifugation to pellet the inclusion bodies, which were then dissolved in 8 M urea, 10 mM Tris/HCl, 1 mM EDTA, pH 8.5 (buffer A). Anion-exchange chromatography was performed in batch mode. The urea-dissolved inclusion bodies were diluted four times with buffer A, and applied to DEAE cellulose resin equilibrated in buffer A. The resin was washed with 20 mM NaCl in buffer A and eluted with 75 mM NaCl in buffer A. The eluted peptide was passed through a 30 kDa molecular weight cutoff (MWCO) filter by centrifugation, and concentrated using a 5 kDa MWCO filter. The peptide was lyophilized and dissolved in 6 M GuHCl, pH 8.5, and monomer was isolated using gel filtration on a 2.6 × 60 cm Superdex75 column (GE Healthcare) in 20 mM sodium phosphate buffer with 0.2 mM EDTA, pH 8.0. The monomer was stored as lyophylized aliquots. Aβ(MC1−42) was purified in the same manner except that 1 mM DTT was present during the sonication steps, and 0.1 mM DTT in the following steps.

Fluorophore Labeling. The Aβ(MC1−42) variant has a cysteine residue incorporated just prior to Asp1 to allow for site-specific labeling at the N-terminus using maleimide chemistry.[22] For each labeling, one aliquot of purified Aβ(MC1−42) was dissolved in 6 M GuHCl pH 8.0 with 1 mM DTT and monomer isolated by size exclusion chromatography in 20 mM sodium phosphate buffer, pH 8.0. AlexaFluor488, AlexaFluor546, or IRDye800 maleimide was dissolved at 5 mM in DMSO, and added to the freshly collected monomers at 2.0 times the monomer concentration. The solution was incubated for 2 h at 4 °C, after which another size exclusion step was performed to eliminate aggregated species and free dye. The concentration of labeled peptide was estimated using the absorbance and the following extinction coefficients: 71 000 $M^{-1}\cdot cm^{-1}$ at 488 nm, 112 000 $M^{-1}\cdot cm^{-1}$ at 546 nm, and 240 000 $M^{-1}\cdot cm^{-1}$ at 800 nm.

Sample Preparation for Array Screening with On-Pathway Oligomers. Just prior to the experiment, purified aliquots of Aβ(M1−42) and Alexa546-Aβ(MC1−42) were dissolved in 6 M GuHCl and subjected to gel filtration and buffer exchange on a 1 × 30 cm Superdex 75 column (GE Healthcare) in 20 mM sodium phosphate buffer, pH 8.0. The monomer fraction was collected in low-binding tubes (Axygen) and kept on ice. For Aβ(M1−42), the monomer concentration was calculated from integration of the collected fraction in the chromatogram using an extinction coefficient at 280 nm of 1440 $M^{-1}cm^{-1}$. For Alexa546-Aβ(MC1−42) the monomer concentration was estimated by recording the absorbance for withdrawn samples (3 × 1 μL) using Nanodrop2000 and an extinction coefficient at of 112 000 $M^{-1}cm^{-1}$ at 546 nm. The monomers were mixed 1:5 Alexa546-Aβ(MC1−42)/Aβ(M1−42) and supplemented with NaCl and KCl from concentrated stocks to achieve 5 μM total monomer concentration in 20 mM sodium phosphate, 137 mM NaCl, 27 mM KCl, pH 8.0 (PBS). The solution was preincubated for 8 min at 37 °C in the low-binding tube in a heating block, and then for an additional 15 min with the array as below.

Array Screening with On-Pathway Oligomers. Human protein microarrays (Protoarray v5.0, Life Technologies) were screened at a constant temperature of 37 °C. Arrays were blocked in 5% milk solids (w/v) in PBS for 60 min followed by a 5 min wash in PBS prior to adding the 8 min preincubated sample on a coverslip, application of a protoarray on top of the solution, and 15 min incubation at 37 °C. Postincubation the microarray was washed for 10 min in PBS. The microarray was dried with centrifugation at 250*g* for 3 min and imaged on a Genepix 4000B scanner (Axon Instruments). The PMT gain settings were maintained at 650 and 300 for the 635 and 532 nm lasers, respectively. The focus position was 10 μm. The microarrays used were all from the same lot. The .gpr result files from the array scans were analyzed with Prospector software (Invitrogen) using protein−protein interaction (PPI) analysis settings.

Array Screening with a Fibrillar Sample. Array screening was performed in exactly the same manner as the on-pathway oligomer sample using a sample with sample with freshly prepared fibrils at 5 μM total monomer concentration and a 1:5 ratio of Alexa546-Aβ(MC1−42)/Aβ(M1−42) in PBS.

Expression and Purification of GSK3α and GSK3β. Human embryonic kidney cells (HEK-293 T) were transiently transfected with pEF1-N-CMV-Tev-GSK3α. Cells were lysed 24 h post-transfection in a high detergent lysis buffer (2 mM $CaCl_2$, 50 mM Tris-HCl, 100 mM NaCl, 0.5% CHAPS (3-[(3-cholamidopropyl)dimethylammonio]-1-propanesulfonate hydrate), 0.1% CHS (cholesteryl hydrogen succinate), 1% DDM (*n*-dodecyl β-D-maltoside), 30% glycerol, and protease inhibitors (Roche)). Cells were cleared by centrifugation at 10 000*g* for 20 min at 4 °C. The purification relies on the Ca^{2+}-dependent high-affinity interaction between EF-hand 1 (EF1) and EF-hand 2 (EF2) of calbindin D_{9k}. EF2-agarose resin specific to EF1 and control beads were incubated with 1.5 mg of EF1-N-GSK3α lysate. Following incubation, samples were collected by centrifugation at 5000*g* for 1 min at 4 °C. EF1-N-GSK3α was eluted from the EF2-agarose beads in elution buffer (10 mM HEPES, 150 mM NaCl, 10 mM EDTA). GSK3β was expressed from a pEF1-N-CMV-Tev-GSK3β vector and purified in the same manner as GSK3α. A second sample of GSK3α was purchased from Origene (TP308698, Rockville) and used in the thermophoresis and kinase assay. A second sample of GSK3β was purchased from Sino Biological (10044-H07B, Beijing) and used in the thermophoresis assay.

Expression and Purification of Control Proteins. Calbindin D_{9k} (bovine minor A with the P43 M mutation) was expressed in *E. coli* and purified as described.[40] EF-hand1 of this protein was prepared by CNBr cleavage followed by ion exchange purification as described.[41]

SPR. The SPR studies were performed using a Biacore 3000 (GE Healthcare, Uppsala, Sweden) instrument, and 10 mM Hepes/NaOH, 0.15 M NaCl, 3 mM EDTA, 0.005% Tween20, pH 7.4 as running buffer at a flow rate of 10 μL/min. Before immobilization, CM5

DOI: 10.1021/acschemneuro.5b00262
ACS Chem. Neurosci. 2016, 7, 161−170

carboxymethylated dextran sensor chips (GE Healthcare, Uppsala, Sweden) were activated by injecting a mixture of 0.2 M 1-ethyl-3-(3-(dimethylamino)propyl)-carbodiimide and 0.02 M *N*-hydroxysuccinimide in water in all four flow channels. To couple Aβ42, 100 μL of a freshly prepared solution of 10 μM monomers in 10 mM sodium acetate buffer pH 3 was injected in channels 2−4. All flow channel were blocked by injecting 70 μL of 1 M ethanolamine; thus, channel 1 was prepared to serve as negative control. To study the association of GSK3α or GSK3β, the kinase was injected at concentration ranging from 1 to 20 nM for 20 min, followed by buffer flow for up to 24 h. To remove background signal the recorded response of the control channel was subtracted from the values obtained from channels with immobilized Aβ42. The presented data are then averaged over channels 2−4. In a control experiment, EF-hand 1 of bovine calbindin D_{9k} (43 residues, net charge −2) was immobilized on a CM5 sensorchip using the same procedure as above. GSK3α was injected over this chip at 20 nM for 20 min, followed by buffer flow.

The dissociation phase data minus baseline were fitted to a single exponential decay:

$$Y = A\ \exp(-k_{off}t)$$

where A is the amplitude and k_{off} is the dissociation rate constant.

The association phase data minus baseline were fitted to a single exponential decay:

$$Y = A(1 - \exp(-(Ck_{on} + k_{off})t))Ck_{on}(Ck_{on} + k_{off})$$

where A is the amplitude, C is the GSK3α concentration in the flow, k_{on} is the association rate constant, and k_{off} is the dissociation rate constant.

Thermophoresis. Just prior to the experiment, purified aliquots of Alexa488-Aβ(MC1−42) were dissolved in 6 M GuHCl and subjected to gel filtration on a Superdex 75 column in 20 mM sodium phosphate buffer, pH 8.0. The monomer fraction was collected in low-binding tubes (Axygen), supplemented with NaCl and KCl from concentrated stocks to achieve 20 mM sodium phosphate, 137 mM NaCl, 27 mM KCl, pH 8.0 (PBS). Two samples were prepared with 60 nM Alexa488-Aβ(MC1−42) monomer, one without GSK3α and one with 188 nM GSK3α in PBS. These two samples were used to prepare 15 samples with logarithmic spacing of the GKS3α concentration between 3.4 and 188 nM. These samples, plus the sample with no GKS3α, were placed in low-binding capillaries (MST Premium Coated from Nanotemper Technologies, München) and mounted in a Monolith NT.115 Instrument (Nanotemper Technologies, München) operated at 37 °C. Thermophoresis measurements were repeated 70 times over a time period of 800 min using LED power 50%, themorophoresis 80%. The data presented in Figure 3A of the main text are from one time point in this series. The therophoresis signal, as a function of total GSK3α concentration, C, in nM, were fitted using a 1:1 binding equation:

$$Y = Y_{free} + (Y_{bound} - Y_{free})X/(X + K_D)$$

$$X = 0.5(C - 60 - K_D) + \sqrt{(0.25(C - 60 - K_D)^2 + CK_D)}$$

where Y is the calculated signal, Y_{free} is its contribution from free Alexa488-Aβ(MC1−42), and Y_{bound} is its contribution from bound Alexa488-Aβ(MC1−42). X is the free GSK3α concentration, C is the total GSK3α concentration in nM, and 60 is the total Alexa488-Aβ(MC1−42) concentration in nM. The potential interactions of Alexa488-Aβ(MC1−42) with GSK3β and Alexa488-Aβ(MC1−42) with calbindin D9k were studied in the exact same manner.

Primary Neurons. The primary mouse neuronal cultures were prepared from cortices and hippocampi of embryonic day 15 mouse embryos as previously described (Takahashi et al. 2004). In brief E15 brain tissue was dissociated by trypsinization and trituration in DMEM with 10% fetal bovine serum (Gibco). Dissociated neurons were cultured on poly-D-lysine (Sigma) coated glass coverslips and were maintained in neurobasal medium (Gibco), B27 supplement (Gibco), glutamine (Invitrogen) and antibiotics (ThermoScientific). All animal experiments were approved by the Animal Ethical Committee of Lund University.

Confocal Microscopy. The cultured primary mouse neurons were fixed at 19 days in vitro (DIV) in 4% formaldehyde in PBS with 0.12 M sucrose for 20 min, permeabilized and blocked in PBS containing 2% normal goat serum (NGS), 1% bovine serum albumin (BSA), and 0.1% saponin (room temperature, 1 h), and then immunolabeled in 2% NGS in PBS overnight at 4 °C with monoclonal anti-Aβ42 antibody 12F4 (Biolegend) and anti-GSKα (Cell Signaling) or anti-GSKβ (Cell Signaling). After labeling with secondary antibodies and appropriate washing, coverslips were mounted with SlowfadeGold (Invitrogen). Images were taken with confocal laser scanning microscopy (Leica TCS SP8) and analyzed with ImageJ and ImarisColoc 7.6. Channels were imaged sequentially to avoid bleed-through.

Cell Culture and Cell Lines for Immunoprecipitation. All cells were cultured in Dulbecco's modified Eagle's medium (DMEM) supplemented with 10% fetal calf serum, 100 units/mL penicillin, and 100 μg/mL streptomycin. Cells were incubated in a humidified incubator set at 5% CO_2, and 37 °C.

Immunoprecipitation. Cells were lysed in 1% (w/v) Triton X-100/PBS before centrifugation, and lysates were then clarified by spinning at 20 000*g* at 4 °C for 10 min. Cleared lysates were then incubated overnight with relevant antibodies (GSK3α, GSK3β (Cell Signaling Technologies) or Aβ (4G8) (Covance)) overnight at 4 °C. Protein A magnetic beads (Cell Signaling Technologies) or Dynabeads M-280 with Sheep anti-rabbit IgG (Invitrogen) were washed in 1% (w/v) Triton X-100/PBS and then blocked for 30 min in 5% skim milk powder before incubation with lysate solution for 1 h at 4 °C. Beads were subsequently isolated on a magnetic rack and washed 6× in 1% (w/v) Triton X-100/PBS and 3× in PBS. For IR800-Aβ42 experiments, IR800-Aβ42 was mixed 1:10 with unlabeled Aβ42 and added to washed beads in PBS to a final concentration of 1 μM, and incubated with the beads for 1 h at 4 °C before washing as described above.

Western Blot. Samples were boiled in Laemmli buffer for 5 min before being applied to 10−20% polyacrylamide gels (BioRad) and subsequent transfer to PVDF membrane using TransBlot Turbo transfer packs (BioRad). Membranes were blocked in 5% skim milk powder. The membranes were incubated in primary antibody (GSK3α, Aβ, Tau (Tau46) (Cell Signaling Technologies), Tau Phospho Ser396 (BD-Bioscience), and Amyloidβ (6E10) (Covance)) solutions overnight. HRP conjugated secondary antibodies were from Cell Signaling Technologies. Protein bands were detected using Signal Fire ECL reagent (Cell Signaling Technologies) and imaged on BioRad ChemiDoc XRS+. Quantification was performed using Image Lab Software (BioRad). Blots with IR labeled proteins were processed using Odyssey CLx Imager (LI-COR Biosciences).

Phosphorylation Assay. Tau phosphorylation assays were performed at 37 °C in 20 mM Tris/HCl, 150 mM NaCl, 20 mM $MgCl_2$, 50 μM DTT, pH 7.5 with 10 μM ATP, and 150 nM tau (T08-54H from SignalChem, Richmond, Canada). For these assays, we used GSK3α from Origene, at a final concentration of 0.2 nM. Just prior to each experiment, a purified aliquot of Aβ(M1−42) was dissolved in 6 M GuHCl and subjected to gel filtration and buffer exchange on a Superdex 75 column in 20 mM Tris/HCl pH 8.0. The monomer fraction was collected in low-binding tubes (Axygen) and kept on ice during adjustment of pH to 7.5, dilution to 5 μM in the reaction buffer. The monomer was incubated at 37 °C for 8 min before adding to the phosphorylation reactions at final concentration of 5, 50, and 500 nM. A control reaction with no Aβ42 was performed in parallel. Another control reaction contained 500 nM Aβ42 but no GSK3α. All solutions were incubated for 45 min at 37 °C. The reactions were stopped by mixing with 2× SDS gel loading buffer and separated on SDS PAGE, followed by Western blots using antibodies against total tau or tau with phospho-Ser396.

DOI: 10.1021/acschemneuro.5b00262
ACS Chem. Neurosci. 2016, 7, 161−170

■ ASSOCIATED CONTENT

Supporting Information

The Supporting Information is available free of charge on the ACS Publications website at DOI: 10.1021/acschemneuro.5b00262.

SPR and thermophoresis control experiments as well as sequence alignment of GSK3α and GSK3β (PDF)

■ AUTHOR INFORMATION

Corresponding Authors

*E-mail: Sara.linse@biochemistry.lu.se.
*E-mail: david.oconnell@ucd.ie.

Author Contributions

‖C.J.D. and G.M.G. contributed equally. S.L. and D.J.O'C. designed the study. S.L., D.J.O'C., C.J.D., G.M.G., and K.W. performed experiments. S.L., D.J.O'C., C.J.D., G.M.G., G.K.G., and K.W. analyzed data. S.L. and D.J.O'C. wrote the paper with input from all coauthors.

Funding

This work was funded by The Swedish Research Council (S.L., G.K.G.), the European Research Council (S.L.), The Swedish Alzheimer Foundation (S.L.), Multipark (S.L., C.J.D.), the Nanometer structure consortium at Lund University (S.L.), JPND (C.J.D., S.L.) Science Foundation Ireland Investigator and TIDA programmes (G.M.G., D.J.O'C.).

Notes

The authors declare no competing financial interest.

■ ABBREVIATIONS

GSK3α, glycogen synthase kinase 3 α; GSK3β, glycogen synthase kinase 3 β; Tris, tris(hydroxymethyl)aminomethane; ATP, adenosine triphosphate; DTT, dithiothreitol; HRP, horseradish peroxidase; EDTA, ethylenediaminetetraacetic acid

■ REFERENCES

(1) Hebert, L. E., Weuve, J., Scherr, P. A., and Evans, D. A. (2013) Alzheimer disease in the United States (2010−2050) estimated using the 2010 census. *Neurology 80*, 1778−1783.

(2) Selkoe, D. J. (2013) The therapeutics of Alzheimer's disease: Where we stand and where we are heading. *Ann. Neurol. 74*, 328−336.

(3) Hardy, J. (2009) The amyloid hypothesis for Alzheimer's disease: a critical reappraisal. *J. Neurochem. 110*, 1129−1134.

(4) Selkoe, D. J. (2013) SnapShot: pathobiology of Alzheimer's disease. *Cell 154*, 468−468.

(5) Citron, M., Oltersdorf, T., Haass, C., McConlogue, L., Hung, A. Y., Seubert, P., Vigo-Pelfrey, C., Lieberburg, I., and Selkoe, D. J. (1992) Mutation of the beta-amyloid precursor protein in familial Alzheimer's disease increases beta-protein production. *Nature 360*, 672−674.

(6) Nilsberth, C., Westlind-Danielsson, A., Eckman, C. B., Condron, M. M., Axelman, K., Forsell, C., Stenh, C., Luthman, J., Teplow, D. B., Younkin, S. G., Näslund, J., and Lannfelt, L. (2001) The 'Arctic' APP mutation (E693G) causes Alzheimer's disease by enhanced Abeta protofibril formation. *Nat. Neurosci. 4*, 887−893.

(7) Di Fede, G., Catania, M., Morbin, M., Rossi, G., Suardi, S., Mazzoleni, G., Merlin, M., Giovagnoli, A. R., Prioni, S., Erbetta, A., Falcone, C., Gobbi, M., Colombo, L., Bastone, A., Beeg, M., Manzoni, C., Francescucci, B., Spagnoli, A., Cantù, L., Del Favero, E., Levy, E., Salmona, M., and Tagliavini, F. (2009) A recessive mutation in the APP gene with dominant-negative effect on amyloidogenesis. *Science 323*, 1473−1477.

(8) Strittmatter, W. J., Saunders, A. M., Schmechel, D., Pericak-Vance, M., Enghild, J., Salvesen, G. S., and Roses, A. D. (1993) Apolipoprotein E: high-avidity binding to beta-amyloid and increased frequency of type 4 allele in late-onset familial Alzheimer disease. *Proc. Natl. Acad. Sci. U. S. A. 90*, 1977−1981.

(9) Cohen, S. I., Linse, S., Luheshi, L. M., Hellstrand, E., White, D. A., Rajah, L., Otzen, D., Vendruscolo, M., Dobson, C. M., and Knowles, T. P. (2013) Proliferation of amyloid-β42 aggregates occurs through a secondary nucleation mechanism. *Proc. Natl. Acad. Sci. U. S. A. 110*, 9758−9763.

(10) Cohen, S. I., Arosio, P., Presto, J., Kurudenkandy, F. R., Biverstål, H., Dolfe, L., Dunning, C., Yang, X., Frohm, B., Vendruscolo, M., Johansson, J., Dobson, C. M., Fisahn, A., Knowles, T. P. J., and Linse, S. (2015) A molecular chaperone breaks the catalytic cycle that generates toxic Aβ oligomers. *Nat. Struct. Mol. Biol. 22*, 207−213.

(11) Arosio, P., Knowles, T. P., and Linse, S. (2015) On the lag phase in amyloid fibril formation. *Phys. Chem. Chem. Phys. 17*, 7606−7618.

(12) Arosio, P., Cukalevski, R., Frohm, B., Knowles, T. P., and Linse, S. (2014) Quantification of the concentration of Aβ42 propagons during the lag phase by an amyloid chain reaction assay. *J. Am. Chem. Soc. 136*, 219−225.

(13) Shen, L., Adachi, T., Van den Bout, D., and Zhu, X. Y. (2012) A mobile precursor determines amyloid-β peptide fibril formation at interfaces. *J. Am. Chem. Soc. 134*, 14172−14178.

(14) Jan, A., Adolfsson, O., Allaman, I., Buccarello, A. L., Magistretti, P. J., Pfeifer, A., Muhs, A., and Lashuel, H. A. (2011) Abeta42 neurotoxicity is mediated by ongoing nucleated polymerization process rather than by discrete Abeta42 species. *J. Biol. Chem. 286*, 8585−8596.

(15) Dubnovitsky, A., Sandberg, A., Rahman, M. M., Benilova, I., Lendel, C., and Hard, T. (2013) Amyloid-β protofibrils: size, morphology and synaptotoxicity of an engineered mimic. *PLoS One 8*, e66101.

(16) Rahman, M., Zetterberg, H., Lendel, C., and Härd, T. (2015) Binding of human proteins to amyloid-β protofibrils. *ACS Chem. Biol. 10*, 766−774.

(17) Koldamova, R. P., Lefterov, I. M., Lefterova, M. I., and Lazo, J. S. (2001) Apolipoprotein A-I directly interacts with amyloid precursor protein and inhibits A beta aggregation and toxicity. *Biochemistry 40*, 3553−3560.

(18) Calero, M., Rostagno, A., and Ghiso, J. (2012) Search for amyloid-binding proteins by affinity chromatography. *Methods Mol. Biol. 849*, 213−223.

(19) Yan, S. D., Chen, X., Fu, J., Chen, M., Zhu, H., Roher, A., Slattery, T., Zhao, L., Nagashima, M., Morser, J., Migheli, A., Nawroth, P., Stern, D., and Schmidt, A. M. (1996) RAGE and amyloid-beta peptide neurotoxicity in Alzheimer's disease. *Nature 382*, 685−691.

(20) Kam, T. I., Song, S., Gwon, Y., Park, H., Yan, J. J., Im, I., Choi, J. W., Choi, T. Y., Kim, J., Song, D. K., Takai, T., Kim, Y. C., Kim, K. S., Choi, S. Y., Choi, S., Klein, W. L., Yuan, J., and Jung, Y. K. (2013) FcγRIIb mediates amyloid-β neurotoxicity and memory impairment in Alzheimer's disease. *J. Clin. Invest. 123*, 2791−2802.

(21) Kim, T., Vidal, G. S., Djurisic, M., William, C. M., Birnbaum, M. E., Garcia, K. C., Hyman, B. T., and Shatz, C. J. (2013) Human LilrB2 is a β-amyloid receptor and its murine homolog PirB regulates synaptic plasticity in an Alzheimer's model. *Science 341*, 1399−1404.

(22) Nasir, I., Linse, S., and Cabaleiro-Lago, C. (2015) Fluorescent Filter-Trap Assay for Amyloid Fibril Formation Kinetics in Complex Solutions. *ACS Chem. Neurosci. 6*, 1436−44.

(23) Lendel, C., Bjerring, M., Dubnovitsky, A., Kelly, R. T., Filippov, A., Antzutkin, O. N., Nielsen, N. C., and Härd, T. (2014) A hexameric peptide barrel as building block of amyloid-β protofibrils. *Angew. Chem., Int. Ed. 53*, 12756−12760.

(24) Colvin, M. T., Silvers, R., Frohm, B., Su, Y., Linse, S., and Griffin, R. G. (2015) High Resolution Structural Characterization of Aβ42 Amyloid Fibrils by MAS NMR. *J. Am. Chem. Soc. 137*, 7509−7518.

(25) Pujol-Pina, R., Vilaprinyó-Pascual, S., Mazzucato, R., Arcella, A., Vilaseca, M., Orozco, M., and Carulla, N. (2015) SDS-PAGE analysis of Aβ oligomers is disserving research into Alzheimeŕs disease: appealing for ESI-IM-MS. *Sci. Rep. 5*, 14809.

DOI: 10.1021/acschemneuro.5b00262
ACS Chem. Neurosci. 2016, 7, 161−170

(26) Citron, M., Oltersdorf, T., Haass, C., McConlogue, L., Hung, A. Y., Seubert, P., Vigo-Pelfrey, C., Lieberburg, I., and Selkoe, D. J. (1992) Mutation of the beta-amyloid precursor protein in familial Alzheimer's disease increases beta-protein production. *Nature 360*, 672−674.
(27) Beurel, E., Grieco, S. G., and Jope, S. (2015) Glycogen synthase kinase-3 (GSK3): Regulation, actions, and diseases. *Pharmacol. Ther. 148*, 114−131.
(28) Medina, M., and Avila, M. J. (2013) Understanding the relationship between GSK-3 and Alzheimer's disease: a focus on how GSK-3 can modulate synaptic plasticity processes. *Expert Rev. Neurother. 13*, 495−503.
(29) Ma, T. (2014) GSK3 in Alzheimer's disease: mind the isoforms. *J. Alzheimer's Dis. 39*, 707−10.
(30) Llorens-Martín, M., Jurado, J., Hernández, F., and Avila, J. (2014) GSK-3β, a pivotal kinase in Alzheimer disease. *Front. Mol. Neurosci. 7*, 46.
(31) Peineau, S., Taghibiglou, C., Bradley, C., Wong, T. P., Liu, L., Lu, J., Lo, E., Wu, D., Saule, E., Bouschet, T., Matthews, P., Isaac, J. T., Bortolotto, Z. A., Wang, Y. T., and Collingridge, G. L. (2007) LTP inhibits LTD in the hippocampus via regulation of GSK3beta. *Neuron 53*, 703−717.
(32) Ma, T., Tzavaras, N., Tsokas, P., Landau, E. M., and Blitzer, R. D. (2011) Synaptic stimulation of mTOR is mediated by Wnt signaling and regulation of glycogen synthase kinase-3. *J. Neurosci. 31*, 17537−17546.
(33) Ishiguro, K., Shiratsuchi, A., Sato, S., Omori, A., Arioka, M., Kobayashi, S., Uchida, T., and Imahori, K. (1993) Glycogen synthase kinase 3 beta is identical to tau protein kinase I generating several epitopes of paired helical filaments. *FEBS Lett. 325*, 167−172.
(34) Phiel, C. J., Wilson, C. A., Lee, V. M., and Klein, P. S. (2003) GSK-3alpha regulates production of Alzheimer's disease amyloid-beta peptides. *Nature 423*, 435−439.
(35) Hurtado, D. E., Molina-Porcel, L., Carroll, J. C., Macdonald, C., Aboagye, A. K., Trojanowski, J. Q., and Lee, V. M. (2012) Selectively silencing GSK-3 isoforms reduces plaques and tangles in mouse models of Alzheimer's disease. *J. Neurosci. 32*, 7392−7402.
(36) Deng, Y., Xiong, Z., Chen, P., Wei, J., Chen, S., and Yan, Z. (2014) β-amyloid impairs the regulation of N-methyl-D-aspartate receptors by glycogen synthase kinase 3. *Neurobiol. Aging 35*, 449−459.
(37) Choi, S. H., Kim, Y. H., Hebisch, M., Sliwinski, C., Lee, S., D'Avanzo, C., Chen, H., Hooli, B., Asselin, C., Muffat, J., Klee, J. B., Zhang, C., Wainger, B. J., Peitz, M., Kovacs, D. M., Woolf, C. J., Wagner, S. L., Tanzi, R. E., and Kim, D. Y. (2014) A three-dimensional human neural cell culture model of Alzheimer's disease. *Nature 515*, 274−278.
(38) Scala, F., Fusco, S., Ripoli, C., Piacentini, R., Li Puma, D. D., Spinelli, M., Laezza, F., Grassi, C., and D'Ascenzo, M. (2015) Intraneuronal Aβ accumulation induces hippocampal neuron hyperexcitability through A-type K(+) current inhibition mediated by activation of caspases and GSK-3. *Neurobiol. Aging 36*, 886−900.
(39) Walsh, D. M., Thulin, E., Minogue, A. M., Gustavsson, N., Pang, E., Teplow, D. B., and Linse, S. (2009) A facile method for expression and purification of the Alzheimer's disease-associated amyloid beta-peptide. *FEBS J. 276*, 1266−1281.
(40) Chazin, W. J., Kördel, J., Drakenberg, T., Thulin, E., Brodin, P., Grundström, T., and Forsén, S. (1989) Proline isomerism leads to multiple folded conformations of calbindin D9k: direct evidence from two-dimensional 1H NMR spectroscopy. *Proc. Natl. Acad. Sci. U. S. A. 86*, 2195−2198.
(41) Finn, B. E., Kördel, J., Thulin, E., Sellers, P., and Forsén, S. (1992) Dissection of calbindin D9k into two Ca(2+)-binding subdomains by a combination of mutagenesis and chemical cleavage. *FEBS Lett. 298*, 211−214.

DOI: 10.1021/acschemneuro.5b00262
ACS Chem. Neurosci. 2016, 7, 161−170